Cold-End Subsystem Testing for the Fission Power System Technology Demonstration Unit

Maxwell Briggs[1], Marc Gibson[1], David Ellis[1], James Sanzi[2]

[1]*Thermal Energy Conversion Branch, NASA Glenn Research Center, Cleveland, OH 44135*
[2]*Vantage Corporation, Cleveland, OH 44135*

Abstract. The Fission Power System (FPS) Technology Demonstration Unit (TDU) consists of a pumped sodium-potassium (NaK) loop that provides heat to a Stirling Power Conversion Unit (PCU), which converts some of that heat into electricity and rejects the waste heat to a pumped water loop. Each of the TDU subsystems is being tested independently prior to full system testing at the NASA Glenn Research Center. The pumped NaK loop is being tested at NASA Marshall Space Flight Center; the Stirling PCU and electrical controller are being tested by Sunpower Inc.; and the pumped water loop is being tested at Glenn. This paper describes cold-end subsystem setup and testing at Glenn. The TDU cold end has been assembled in Vacuum Facility 6 (VF 6) at Glenn, the same chamber that will be used for TDU testing. Cold-end testing in VF 6 will demonstrate functionality; validated cold-end fill, drain, and emergency backup systems; and generated pump performance and system pressure drop data used to validate models. In addition, a low-cost proof-of concept radiator has been built and tested at Glenn, validating the design and demonstrating the feasibility of using low-cost metal radiators as an alternative to high-cost composite radiators in an end-to-end TDU test.

INTRODUCTION

The Fission Power System (FPS) team is developing technologies for an affordable FPS to support future exploration missions. The FPS Initial Concept Definition (Fission Surface Power Team (2011)) is based on surface power applications, using a below-grade reactor and vertical truss to support balance-of-plant (BOP) components. The FPS uses a single fast-spectrum uranium dioxide reactor to heat a liquid sodium-potassium (NaK) eutectic. Two fully redundant Annular Linear Induction Pumps (ALIPs) are used to circulate the NaK to a pair of intermediate heat exchangers (IHX). The IHX is a NaK-to-NaK heat exchanger that provides a buffer between the reactor and the BOP. Each of the two intermediate NaK loops service two Power Conversion Units (PCUs). There are four water heat rejection loops (one for each PCU) that transfer the waste heat to two radiator wings (two loops per wing) (Fig. 1). A more detailed description of the FPS reference concept is given in Briggs (2012a).
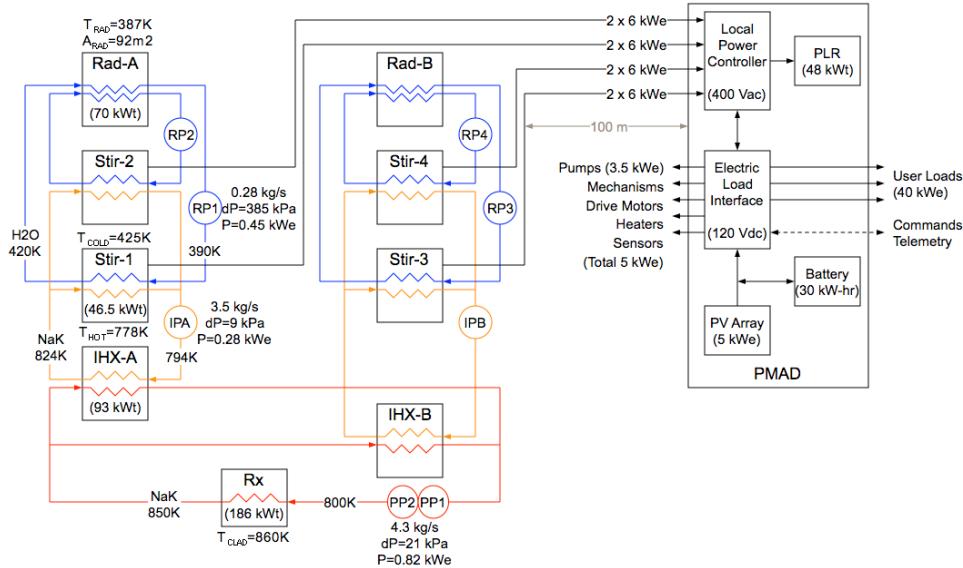
Figure 1.—Original fission power system design schematic.

The FPS Technology Demonstration Unit (TDU) was designed to raise the technology readiness level (TRL) of FPS technology by demonstrating end-to-end system performance and robustness in a relevant environment. The original TDU design included prototypic versions of all major FPS components, excluding the nuclear reactor as shown in Figure 2 (Mason (2006)). In the original design, an electrically heated core simulator provided heat to the primary liquid metal loop, which was pumped using an ALIP. The primary liquid metal loop flowed through an IHX to a secondary liquid metal loop, which transferred the heat to the Stirling hot-end heat exchanger. The PCU converted some of the heat into electricity and rejected waste heat to a pumped water loop. This water loop exchanged heat with six full-scale FPS radiator panels, which radiated the waste heat to the thermal vacuum environment.

Budget reductions have driven many design changes in the TDU over the past few years, reducing the scope of the TDU and preventing the TDU from achieving the originally intended goal of being an end-to-end system-level demonstration (Mason et al. (2011) and Briggs (2012b)). Radiators and the intermediate liquid metal loop were removed completely from the TDU (Fig. 3). In lieu of radiators, the current TDU design rejects waste heat from the Stirling convertors by flowing cooling water outside of the vacuum chamber to a liquid-to-forced air heat exchanger called the Waste Heat Exchanger (WHX). The response of the forced air heat exchanger is fundamentally different from the response of a radiator, so temperature feedback and thermal transients in the new TDU design will be substantially different from those expected in a flight-like FPS.
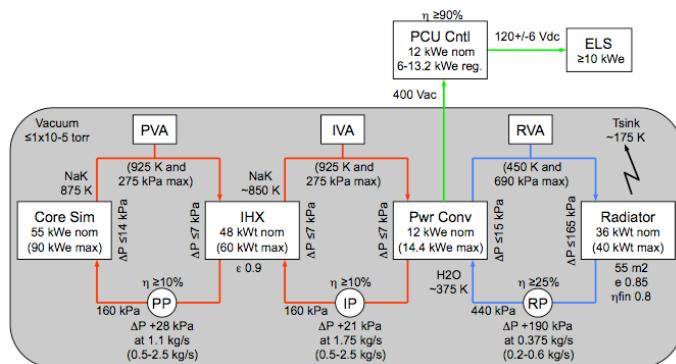

Figure 2.—Original Technology Demonstration Unit design schematic.

η ≥90%

PCU Cntl
12 kWe nom
6-13.2 kWe reg.

120+/-6 Vdc

ELS
≥10 kWe

400 Vac

Waste heat
rejected to
ambient air

Vacuum
≤1x10-5 torr

PVA

RVA

NaK
850 K

(925 K and
275 kPa max)

(450 K and
690 kPa max)

Core Sim
48 kWe nom
(90 kWe max)

ΔP ≤14 kPa

ΔP ≤7 kPa

Pwr Conv
12 kWe nom
(14.4 kWe max)

ΔP ≤15 kPa

Waste Heat
Exchanger

η ≥10%

H2O
~375 K

η ≥25%

160 kPa

PP

ΔP +28 kPa
at 1.75 kg/s
(0.5-2.5 kg/s)

440 kPa

RP

ΔP +190 kPa
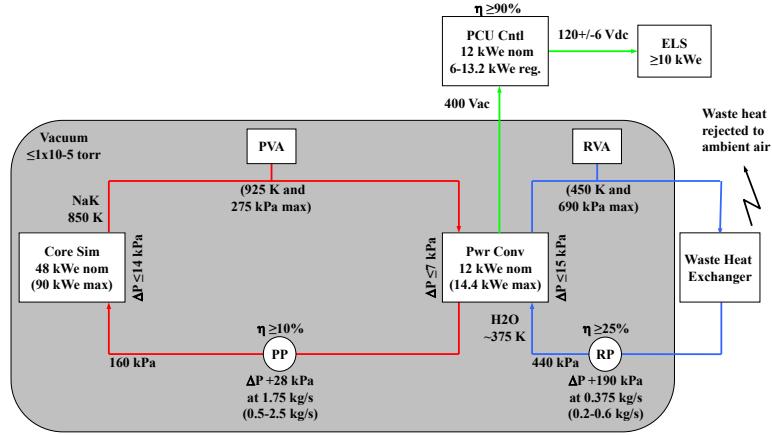at 0.375 kg/s
(0.2-0.6 kg/s)

Figure 3.—Current Technology Demonstration Unit design schematic.

The three major TDU subsystems are the hot end, the PCU, and the cold end. Prior to assembly and testing of the full TDU at Glenn, each of the subsystems is undergoing independent testing. The hot end, referred to as the RxSim, has already been tested at Marshall. The Stirling PCU, controller, and PMAD are being tested at Sunpower, Inc. The cold-end Heat Rejection System (HRS) is being tested at Glenn and is the subject of this paper. HRS testing will verify functionality, validate operating procedures, and document component performance. Additional component level testing has been completed on an affordable, proof-of-concept radiator design, which could potentially provide a cost-effective option for restoring realistic thermal transients and thermal feedback to the TDU cold end.

Heat Rejection System

Heat Rejection System Test Design

The HRS consists of a commercial-off-the-shelf hermetically sealed water pump, a volume accumulator used to accommodate thermal expansion of the water and control loop pressure, and a WHX (Fig. 3). During TDU testing, the PCU would transfer 36 kW_t of heat to the water through the Stirling rejector. This heat would then be rejected through the WHX. During HRS subsystem testing at Glenn, the PCU will not be in the loop, so the heat load on the water comes only from pump inefficiency and fluid friction through the loop, estimated to be less than 1 kW_t. The WHX rejects more than 1 kW_t even with the fan turned off, which would prevent the water loop from reaching the nominal operating temperature. To reach the nominal operating temperature, the WHX has been replaced with a temperature control loop for HRS subsystem testing. The temperature control loop consisted of an oil heater/cooler coupled to the water loop through a plate-fin heat exchanger. Since the WHX has already been successfully tested at the component level removing it from HRS testing was not a concern.

The HRS test will verify functionality and performance of the major TDU components over a wide range of conditions. All support systems, including the fill and drain system, emergency backup water system, nitrogen cover gas regulation, and instrumentation/data acquisition system will be tested. Procedural tests, such as fill/drain and emergency cooling will be performed at atmospheric temperature and pressure. All performance data will be collected at a pressure $<10^{-6}$ torr. Finally, the entire loop will be run through a range of operating conditions in a thermal vacuum environment ($<10^{-6}$ torr < 100 K cold wall temperature).

The HRS components have been mounted to the Upper Truss Structure (UTS), which is the structure that will house all of the TDU components during the full system-level test. Figure 4 shows the HRS components mounted on the UTS and assembled in VF 6 at NASA Glenn. A nitrogen line plumbed to the top of the volume accumulator provides a cover pressure to prevent flashing and cavitation. Water leaving the HRS pump flows to the temperature control loop, which has been assembled outside VF 6 (Fig. 5) before being returned to the pump inlet. The pump

will be operated in a vacuum environment across a range of flow rates (by varying pump speed) and pressure drops (by adjusting a throttling valve), and water temperatures to document pump performance through the entire range of expected operating conditions.

Figure 4.—Heat Rejection System and Upper Truss Structure Vacuum Facility 6.

Figure 5.—Temperature control loop.

Affordable Radiator

Radiator Design and Fabrication

Several different combinations of component materials and layouts were considered for the affordable radiator design, including high-conductivity composite facesheets, low-conductivity composite facesheets, aluminum facesheets, graphite foam saddles, and aluminum saddles. Both single facesheet and dual facesheet configurations were evaluated. Panel geometry and the number of required heat pipes were chosen using an optimization routine to minimize mass for each configuration, allowing for radiator surface area margin. Table I compares the results of the optimized designs.

Table 1.—Comparison of Optimized Radiator Designs

Description	Fin Thickness (mm)	Fin Length (mm)	Two-Sided Area (m^2)	Total Mass (kg)	Estimated Relative Cost*
Dual – High Conductivity Composite Facesheet – Poco Saddles	0.5	200	45.2	90.7	1
Single – High Conductivity Composite Facesheet	0.5	150	50.0	47	.35
Single – Low Conductivity Composite Facesheet	0.5	100	48.4	53.9	.33
Single – Aluminum Facesheet	0.5	100	48.4	65.3	.18
Dual – Low Conductivity Composite Facesheet– Poco Saddles	0.5	200	47.9	95.9	.88
Dual – Low Conductivity Composite Facesheet – Aluminum Saddles	1	200	44.3	265	.63
Dual – Aluminum Facesheet – Aluminum Saddles	.5	200	47.9	266	.30

The clear cost winner in this trade study was the single aluminum facesheet design. Single aluminum facesheet designs force all of the heat through a single lower conductivity facesheet, resulting in steeper temperature gradients

in the fin than those seen in dual composite facesheet designs. Consequently, the optimization routine converged on a design with reduced fin length, more required heat pipes, and a larger overall surface area to reject 36 kW$_t$. Although the increase in the number of heat pipes and overall surface area negatively affected radiator mass, the elimination of saddles and one facesheet compensates for this. This trade study and preliminary design showed that single aluminum facesheet designs have the potential to reduce material costs by a factor of five and decrease overall radiator mass compared to the original high-conductivity composite dual facesheet design (Briggs (2012a)).

This conceptual design for the affordable TDU radiator was used as the basis for a subscale proof-of-concept design, focused on process simplification, cost reduction, and extensibility to full-size TDU panels. The proof-of-concept radiator (Fig. 6) consisted of three titanium-water heat pipes coupled to two redundant water loops through a conductive aluminum manifold block. The heat pipes were bonded directly to four 12- by 18-in. fins, with fin thickness and fin length determined by the affordable radiator conceptual design (Table 1).
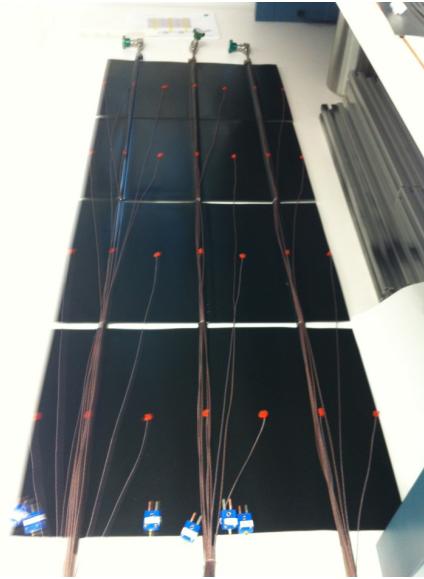

Figure 6.—Proof-of-concept radiator.

The Second Generation (2nd Gen) Radiator Demonstration Unit (RDU) (Ellis et al. (2011)) was a full-scale prototype radiator built by Material Innovation, Inc., and tested at Glenn. The 2nd Gen RDU manifold design flowed water directly over vertical heat pipe evaporators to maximize thermal performance. This method required that each heat pipe be welded to the manifold and required complicated and heavy tubing runs (Fig. 7) to compensate for CTE mismatch between the manifold and the facesheet. The proof-of-concept radiator design sacrifices optimal thermal performance for simplicity, as shown in Figure 8. The heat pipes' evaporators are horizontal so that straight tubing runs could be used in the manifold. The water lines and heat pipe evaporators are conductively coupled through an aluminum manifold block, eliminating the need for welding. The design relies upon clamping rather than adhesive bonding or brazing. Thermal grease minimizes the thermal resistance across the interfaces and allows slippage so that thermal expansion in the manifold does not induce stress in the facesheet. The conductively coupled manifold design has the additional benefit of allowing all heat pipes to remain active even if one water line was lost.
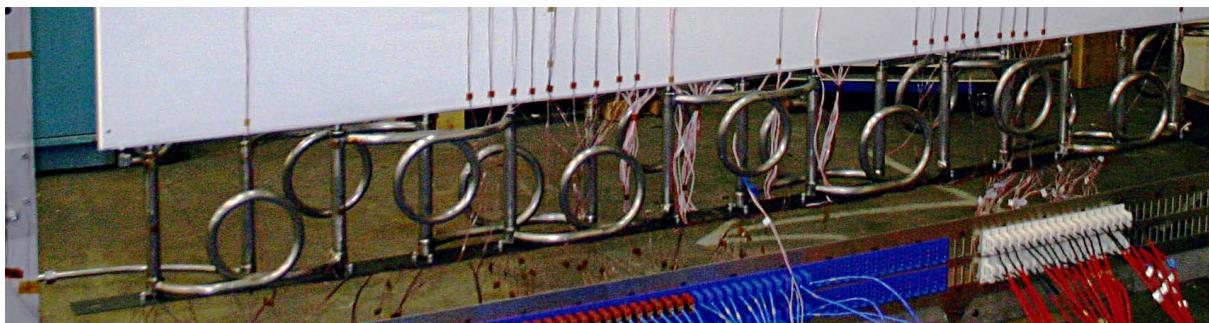
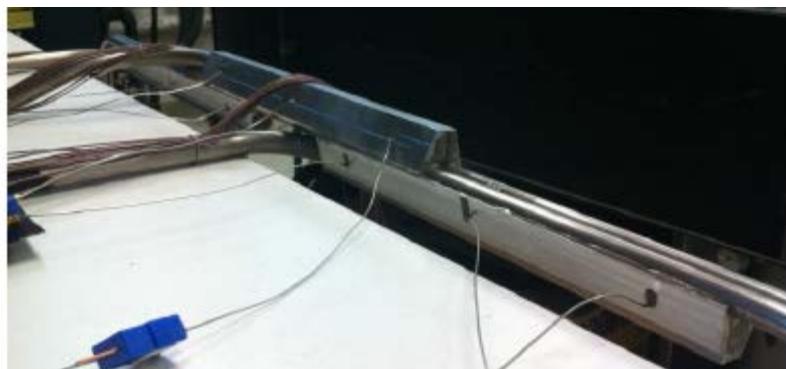Figure 7.—Second Generation Radiator Demonstration Unit manifold.

Figure 8.—Proof-of-concept radiator manifold.

Both adhesive bonding and brazing were considered for joining aluminum facesheets to the titanium heat pipes. Brazing was the clear winner from a performance standpoint as it resulted in a stronger and more highly conductive bond. However, pressurized heat pipes cannot be put into a brazing oven, which complicates radiator assembly. In addition, finding a brazing furnace capable of brazing full-scale TDU radiator panels could be cost prohibitive, so adhesive bonding was chosen. Several adhesives were considered, including two-part epoxies, some with silver additions for improved thermal conductivity, and structural film adhesives. Each of the epoxies and film adhesives that were considered had cure temperatures below the operating temperature of the heat pipe. This is important because the adhesive can be cured by running the heat pipe, eliminating the need for large-scale ovens. In addition, curing near the operating temperature reduces the thermally induced stress during operation where the adhesives are weakest, and raises the thermally induced stress at room temperature where the adhesives are strongest.

Several candidate adhesives were tested to identify viable candidates. Each adhesive was cured, thermal cycled in a rough vacuum, and single lap shear tested at Glenn to identify viable candidates for this application. The adhesive processing and material testing are discussed in more detail in Ellis et al. (2013). These tests showed that the two-part epoxies typically failed in the 700 to 3500 kPa range, well below the manufacturer's published shear stress. The structural film adhesives had shear strengths in excess of 10 000 kPa. The shear strength of these bonds was likely higher, but substrate yielded, making it impossible to measure higher lap shear strengths. Since the thickness of the substrate is an integral part of the thermal stress calculation, it was not possible to increase the substrate thickness to prevent yielding and measure the true shear strength of the adhesive. The lack of failure of the bond at the yield load of the substrate showed that there will be strain relief, in the form of facesheet or heat pipe yielding, prior to failure of the adhesive. This makes structural adhesives a viable option, even though they are relatively poor thermal performers. The structural adhesives were also easier to apply and cure, which improved manufacturability, the other key issue in reducing cost.

Affordable Radiator Test Results

The proof-of-concept radiator was designed to be simpler, lighter, and more affordable than the 2nd Gen RDU. However, testing was required to demonstrate performance and determine if the structural adhesive could handle the CTE mismatch between the titanium heat pipe and the aluminum facesheet. The panel was tested at water temperatures ranging from 330 to 400 K and a sink temperature of 190 K. At the nominal TDU water inlet temperature of 400 K and flow rate of 0.375 kg/s the 1.1 m^2 panel (two-sided area) rejected 620 W of heat, for a heat rejection per unit area of 570 W/m^2. For comparison purposes the full-scale 2nd Gen RDU panel rejected 760 W/m^2 when operating at similar conditions (Ellis et al. (2011)). The lower heat rejection per unit area of the proof-of-concept radiator is due to larger temperature drops through the conductively coupled manifolds, and steeper temperature gradients along the aluminum fin. This decrease was expected (Briggs (2012a)) and deemed acceptable given the estimated reductions in cost and mass. When these radiators are compared on a mass basis, the 2.0-kg affordable radiator rejected 300 W/kg compared to 240 W/kg for the 30-kg 2nd Gen RDU. Additional heat pipes could be added to the affordable radiator design (decreased fin length) in order to reduce area at the expense of mass as needed to meet TDU requirements.

CONCLUSION

The Fission Power System team at NASA Glenn Research Center is near the end of the buildup for the Heat Rejection System (HRS) subsystem. All components have been mounted to the Technology Demonstration Unit structural elements and have been assembled in the Vacuum Facility 6 test chamber at Glenn. HRS testing will include performance testing of the pump in a vacuum environment and functionally testing the entire subsystem in a thermal vacuum environment. Additional testing has been completed on a proof-of-concept radiator that could offer an affordable alternative to dual high-conductivity composite facesheet designs, which have become cost prohibitive due to budget reductions. The affordable design was shown to increase heat rejection per unit mass compared to the Second Generation Radiator Demonstration Unit at a fraction of the cost.

REFERENCES

Briggs, M. (2012a): Conceptual Design of an Affordable Radiator for the Fission Power System Technology Demonstration Unit. NETS 2012, Paper 3031.

Briggs, M., et al. (2012b): Development Status of the Fission Power System Technology Demonstration Unit. NASA/TM—2012-217717, AIAA Paper 2012–3711.

Fission Surface Power Team (2010): Fission Surface Power System Initial Concept Definition. NASA/TM—2010-216772.

Ellis, D.; Briggs, M.; and McGowan, R. (2013): Lap Shear Testing of Candidate Radiator Panel Adhesives. NETS 2013.

Ellis, D.; Calder, J.; and Siamidis, J. (2011): Summary of the Manufacture, Testing and Model Validation of a Full-Scale Radiator for Fission Surface Power Applications. NETS 2011, Paper 3181.

Mason, L., et al. (2011): Design and Test Plans for a Non-Nuclear Fission Power System Technology Demonstration Unit. NASA/TM—2011-217100, NETS–2011–3327.

Mason, L. (2006): A Practical Approach to Starting Fission Surface Power Development. NASA/TM—2006-214366.